the pK_a values of solvents (H_2O (15.7), CH_3OH (16), CH_3COCH_3 (20), C_6H_6 (37))[11] are much larger than that of **3** (11.6 in aqueous solution).[4]

Acknowledgment. We thank the Korea Science and Engineering Foundation and the Ministry of Education for their financial support to this study.

Registry No. 1, 32334-52-4; **2**, 513-42-8; **3**, 56640-70-1; **4**, 78-84-2; deuterium, 7782-39-0.

Thermodynamics of Kinetically Irreversible Organometallic Processes. Metal-Metal Bonds

J. Richard Pugh and Thomas J. Meyer*

Department of Chemistry, The University of North Carolina at Chapel Hill Chapel Hill, North Carolina 27599-3290

Received July 5, 1988

Organometallic chemistry is rich in descriptive chemistry but often lacking in quantitative insight.[1] For oxidation-reduction reactions such as (1) and (2), kinetic irreversibility precludes the

$$Mn_2(CO)_{10} + 2e^- \rightarrow 2Mn(CO)_5^- \quad (1)$$

$$Ir(PPh_3)_2(CO)Cl + 2Cl^- \rightarrow Ir(PPh_3)_2(CO)Cl_3 + 2e^- \quad (2)$$

direct measurement of free energy changes by standard electrochemical techniques. One approach to the evaluation of thermodynamic parameters is by redox equilibration experiments. This approach has been used previously in other areas of research,[2] and we apply it here to obtain quantitative information for oxidation-reduction reactions involving metal-metal bonds.

In the equilibration experiments we utilized a series of couples based on polypyridyl complexes of Ru and Os, such as $[Ru(bpy)_3]^{3+/+}$, $[Ru(bpy)_3]^{2+/+}$ (bpy = 2,2'-bipyridine), or bipyridinium ions such as $TQ^{2+/+}$ (TQ^{2+} = 7,8-dihydro-6*H*-dipyrido[1,2-*a*:2',1'-*c*][1,4]diazepinediium dication).[3] When taken

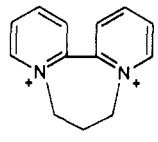

TQ^{2+}

together the couples extend over a range of >3 V in increments of ~50 mV. The IR spectra in the ν_{CO} region in Figure 1 show that the $TQ^{2+/+}$ couple ($E^{\circ\prime}$ = -0.55 V vs SSCE) reaches equilibrium with the $Mn_2(CO)_{10}/2[Mn(CO)_5]^-$ couple in 0.5 M $[N(n\text{-}Bu)_4](PF_6)$-CH_3CN at room temperature. Integration of the ν_{CO} peaks for $Mn_2(CO)_{10}$ and $[Mn(CO)_5]^-$ compared to predetermined calibration curves give K (22 ± 2 °C) = 1.6(±0.3) × 10^{-5} for reaction 3 and $E^{\circ\prime}$ = -0.69(±0.01) V (vs SSCE) for the couple in reaction 4.

$$Mn_2(CO)_{10} + 2TQ^+ \rightleftharpoons 2[Mn(CO)_5]^- + 2TQ^{2+} \quad (3)$$

$$Mn_2(CO)_{10} + 2e^- \rightleftharpoons 2[Mn(CO)_5]^- \quad (4)$$

Fast scan cyclic voltammetry was performed at 10 μm diameter platinum disk microelectrodes at a scan rate of 5000 V/s with potentials recorded in V vs SSCE. In 0.5 M $[N(Bu)_4](PF_6)$-CH_3CN the two-electron reduction of $Mn_2(CO)_{10}$ to $[Mn(CO)_5]^-$

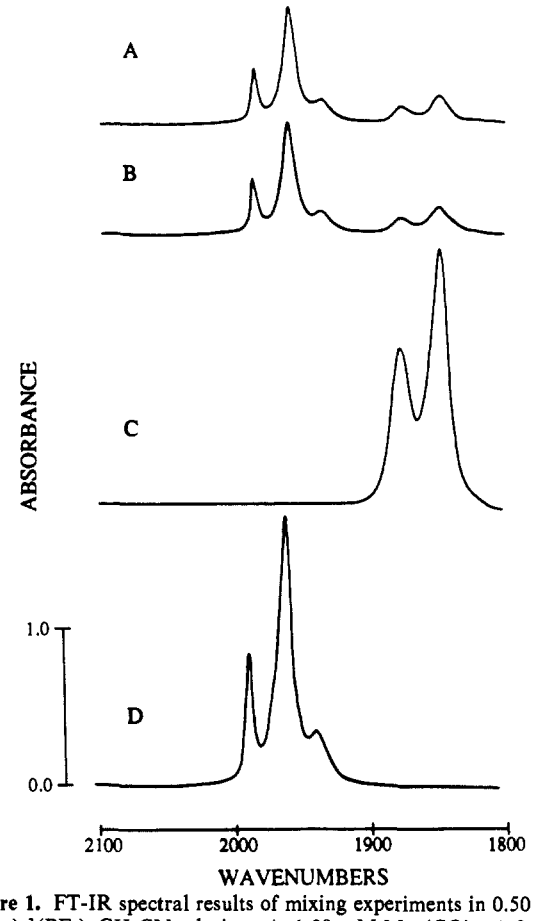

Figure 1. FT-IR spectral results of mixing experiments in 0.50 M $[N(n\text{-}Bu)_4](PF_6)$-CH_3CN solution: A, 1.28 mM $Mn_2(CO)_{10}$ + 2.58 mM TQ^+; B, 2.56 mM $[Mn(CO)_5]^-$ + 2.58 mM TQ^{2+}; C, 5.12 mM $[Mn(CO)_5]^-$; D, 2.56 mM $Mn_2(CO)_{10}$.

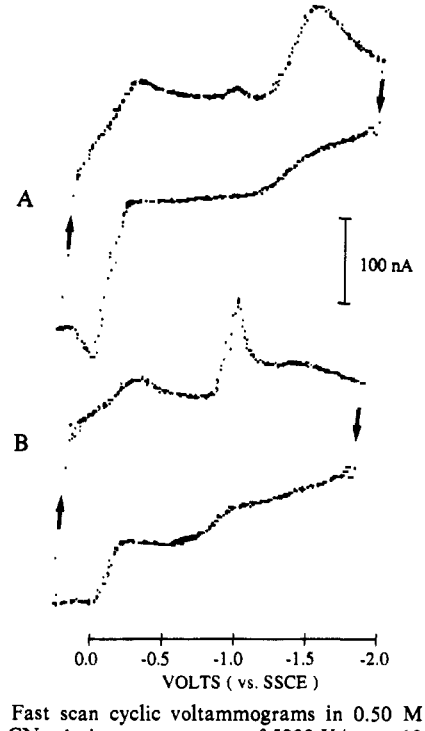

Figure 2. Fast scan cyclic voltammograms in 0.50 M $[N(n\text{-}Bu)_4](PF_6)$-CH_3CN solution at a scan rate of 5000 V/s at a 10 μm diameter platinum disk microelectrode: A, 5.0 mM $Mn_2(CO)_{10}$; B, 5.0 mM $[Mn(CO)_5(NCCH_3)](PF_6)$.

appears at $E_{p,c}$ = -1.50 V (Figure 2A) and is followed by a reversible wave for the $[Mn(CO)_5]^-/Mn(CO)_5$ couple at $E^{\circ\prime}$ = -0.15 V. In addition, a wave for the reduction of $[Mn(CO)_5(NCCH_3)]^+$ is seen at $E_{p,c}$ = -1.10 V. The cation, $[Mn(CO)_5$-

(1) For a review of thermodynamic aspects of organometallic chemistry, see: Connor, J. A. *Topics Curr. Chem.* **1977**, *71*, 71.

(2) (a) Conant, J. B.; Lutz, R. E. *J. Am. Chem. Soc.* **1923**, *45*, 1047-1060. (b) Latimer, W. M. *The Oxidation States of the Elements and Their Potentials in Aqueous Solution*, 2nd ed.; Prentice-Hall: Edgewood, NJ, 1952. (c) Wilson, D. F.; Dutton, P. L.; Erecinska, M.; Lindsay, J. G.; Sato, N. *Acc. Chem. Res.* **1972**, *5*, 234-241.

(3) (a) Homer, R. F.; Tomlinson, T. E. *J. Chem. Soc.* **1960**, 2498. (b) Salmon, R. T.; Hawkridge, F. M. *J. Electroanal. Chem. Interfacial Electrochem.* **1980**, *112*, 253.

0002-7863/88/1510-8245$01.50/0

Scheme I[a]

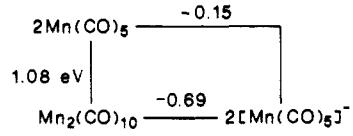

[a] 0.5 M TBAH-CH_3CN solution, 22 ± 2 °C, in V vs SSCE.

Scheme II[a]

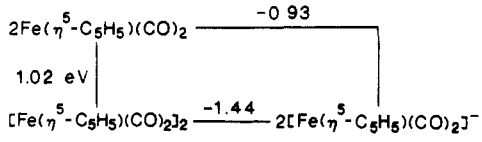

[a] 0.5 M TBAH-CH_3CN solution, 22 ± 2 °C, in V vs SSCE.

$(NCCH_3)]^+$, is formed by a two-electron oxidation of $[Mn(CO)_5]^-$ which is in competition with the one-electron oxidation to give $Mn(CO)_5$. At scan rates lower than ~5000 V/s, dimerization of $Mn(CO)_5$ to give $Mn_2(CO)_{10}$ occurs, and the reductive wave at $E_{p,c} = -0.30$ V is not observed. The large ΔE_p value for the $[Mn(CO)_5]^-/Mn(CO)_5$ couple is a consequence of the high scan rates. Figure 2B shows that reduction of $[Mn(CO)_5(NCCH_3)]^+$ results in the appearance of the $[Mn(CO)_5]^-/Mn(CO)_5$ couple. It also shows that a competition exists between the two-electron reduction of the cation to $[Mn(CO)_5]^-$ at $E_{p,c} = -1.10$ V and one-electron reduction to $Mn(CO)_5$ followed by dimerization and reduction of $Mn_2(CO)_{10}$ at $E_{p,c} = -1.50$ V.[4]

The results of the fast scan and equilibration experiments allow the construction of the Latimer-type diagram in Scheme I. A value of $\Delta G^{\circ\prime}_{M-M} = 25(\pm 1)$ kcal/mol ($K = 5.3 \times 10^{-19}$) for the metal-metal bond equilibrium in reaction 5 can be calculated from the potentials for the monomeric and dimeric couples. Given the expected positive entropy change for reaction 5, this value is in a range consistent with ΔH values for the same equilibrium estimated by other techniques.[5]

$$Mn_2(CO)_{10} \rightleftharpoons 2Mn(CO)_5 \qquad (5)$$

The same electrochemical techniques have been applied to the carbonyl bridged dimer $[Fe(\eta^5\text{-}C_5H_5)(CO)_2]_2$. For the $[Fe(\eta^5\text{-}C_5H_5)(CO)_2]_2/2[Fe(\eta^5\text{-}C_5H_5)(CO)_2]^-$ couple an equilibrium is reached with the $[Ru(bpy)_3]^{2+/+}$ couple ($E^{\circ\prime} = -1.35$ V vs SSCE) with $K(22 \pm 2\ ^\circ C) = 7.8(\pm 0.6) \times 10^{-4}$. From that result and the results of fast scan cyclic voltammetry, $\Delta G^{\circ\prime} = 22(\pm 1)$ kcal/mol ($K = 1.7 \times 10^{-17}$) for the associated metal-metal bond equilibrium in Scheme II.

Until now, the direct measurement of metal-metal bond strengths in solution has been confined to those cases where the metal-metal bond is sufficiently weak to allow the dimer and the associated radicals to establish a detectable equilibrium at room temperature.[6,7] The combination of redox equilibration and fast scan cyclic voltammetry experiments promises to be a more general approach and to allow for the determination of metal-metal bond strengths in solution for cases which are otherwise immeasurable. It also seems clear that the same approach may be of value in establishing thermodynamic redox potentials for other kinetically irreversible organometallic couples.

Acknowledgment. We gratefully acknowledge the support of the Office of Naval Research. We also thank Drs. B. P. Sullivan, M. R. M. Bruce, and A. J. Downard for their helpful discussions.

(4) Lacombe, D. A.; Anderson, G. P.; Kadish, K. M. *Inorg. Chem.* **1986**, *25*, 2074-2079.
(5) (a) Hughey, J. L.; Anderson, C. P.; Meyer, T. J. *J. Organomet. Chem.* **1977**, *125*, C49-50. (b) Haines, L. I. B.; Hopgood, D.; Poë, A. J. *J. Chem. Soc. A* **1968**, 421-428. (c) Marcomini, A.; Poë, A. J. *J. Chem. Soc., Dalton Trans.* **1984**, 95-97. (d) Goodman, J. L.; Peters, K. S.; Vaida, V. *Organometallics* **1986**, *5*, 815-816. (e) Simoes, J. A. M.; Schultz, J. C.; Beauchamp, J. L. *Organometallics* **1986**, *4*, 1238-1242. (f) Cutler, A. R.; Rosenblum, M. *J. Organomet. Chem.* **1976**, *120*, 87-96.
(6) Meyer, T. J. *Prog. Inorg. Chem.* **1975**, *19*, 1-49.
(7) McLain, S. J. *J. Am. Chem. Soc.* **1988**, *110*, 643.

Methyl Chymotrypsin Catalyzed Hydrolyses of Specific Substrate Esters Indicate Multiple Proton Catalysis Is Possible with a Modified Charge Relay Triad[1]

Jeffrey D. Scholten, John L. Hogg,* and Frank M. Raushel*

Department of Chemistry, Texas A&M University
College Station, Texas 77843

Received July 6, 1988

Methyl chymotrypsin, alkylated at $N^{\epsilon}2$ of His-57, still exhibits multiple proton catalysis for the hydrolysis of specific substrate esters even though the classical charge-relay mechanism, long thought to be important for serine protease catalysis, is clearly precluded from operating. The status of the mechanism of serine protease catalysis thus remains in question.[2,3] The charge-relay mechanism, involving multiple proton transfer between Asp-102 and His-57 and between His-57 and Ser-195 or water, has previously been supported by proton inventory studies[4] which have shown multiple proton catalysis for specific substrates.

α-Chymotrypsin has been chemically modified by using methyl *p*-nitrobenzenesulfonate which has been shown to be specific for methylation at $N^{\epsilon}2$ of His-57.[5] The catalytic activity of the methylated enzyme is reduced by a factor of 10^3-10^4 relative to native enzyme.[6] Any catalytic contribution from native enzyme was avoided through the use of the proflavin displacement technique.[6] Since this method allows one to observe only decay of the acyl methyl chymotrypsin there is no possible interference from any contaminant of native enzyme. Alkylation was expected to disrupt the charge-relay triad in such a way as to prevent the multiple proton catalysis indicated by proton inventories with the native enzyme.[4] However, the proton inventory for the deacylation of *N*-acetyl-L-Tyr-methyl chymotrypsin is clearly bowl-shaped (Figure 1 and Table I) and indicates multiple proton catalysis is still being employed ($^Dk_3 = 3.7$). Proton inventories (not shown) for the deacylation of *N*-Cbz-L-Tyr-methyl chymotrypsin and *N*-acetyl-L-Phe-methyl chymotrypsin are also bowl-shaped and exhibit equally large solvent isotope effects. These proton inventories do not become linear, as one might have predicted, with the alkylated enzyme. This indicates that the alkylated enzyme does not simply react by a mechanism in which the Nδ1 of imidazole has moved into a position to abstract a proton from the nucleophilic water molecule involved in hydrolysis of the acyl enzyme. Such a mechanism would produce a linear proton inventory. The observation of multiple proton catalysis suggests that other mechanisms must be considered. The proton inventory can be successfully reproduced[7] (Table I) by using models involving either two-proton or three-proton catalysis. A possible two-proton mechanism is shown in Figure 2, and a three-proton mechanism is shown in Figure 3.

We favor the three-proton model with contributions from H_a and two H_b protons from the oxyanion hole in Figure 3. Fink[2] has recently discussed the importance of the so-called oxyanion hole in catalysis, and this result lends support to his arguments. Arguments[4] which have been used to explain the activation of the charge-relay mechanism dependent on substrate structure may also be used to explain the activation of a mechanism involving the amide protons of the oxyanion hole. We have previously

(1) Abbreviations: methyl chymotrypsin: $N^{\epsilon}2$-His-57 methyl α-chymotrypsin; Tyr: tyrosine; Phe: phenylalanine; Cbz: carbobenzoxy; Asp: aspartic acid; His: histidine.
(2) Fink, A. L. In *Enzyme Mechanisms*; Page, M. I., Williams, A., Eds.; Royal Society of Chemistry: London, 1987; Chapter 10.
(3) Schowen, R. L. In *Principles of Enzyme Activity*; Liebman, J. F., Greenbaum, A., Eds.; VCH Publishers, Inc.: FL, in press.
(4) Schowen, R. L.; Venkatasubban, K. S. *CRC Crit. Rev. Biochem.* **1984**, *17*, 1-44.
(5) Nakagawa, T.; Bender, M. L. *Biochemistry* **1970**, *9*, 259.
(6) Henderson, R. *Biochem. J.* **1971**, *124*, 13.
(7) While the exact fractionation factors (φ) may be varied slightly to give a better numerical fit, the curvature of the inventory plot is the most interesting result, and the exact magnitude of the fractionation factors is not a key issue here. Other models may also reproduce the data.

0002-7863/88/1510-8246$01.50/0